Camera Noise Analysis for Pixel 4a

(**Teachers' Note**: Some of these noise estimates may be a little too high (PRNU, DSNU). The reason is that when using a light the lens shading introduces significant variation across the pixels. This makes the variance a little higher than it should be. This group and last year's group both found that read noise in green is higher than read noise in blue or red. Averaging the two greens brings them into agreement. Surprised!)

Contents:

Introduction

Understanding sensor noise is important as it allows camera designers to investigate the relative influence of different types of noise to help guide their design decisions. In this project we characterized the sensor noise for the Google Pixel 4a camera. The sensor used in the Google Pixel 4a is the 12MP IMX363, manufactured by Sony. We considered read noise and dark noise and two types of fixed-pattern noise, PRNU and DSNU.

Background

Fixed Pattern Noise

Fixed-pattern noise (FPN) is the result of variations in device parameters in the image sensor array itself. It results in spatial variations in the output values of pixels across the image sensor. FPN is present in both the presence of light and the absence of light. Here, we look at two types of fixed-pattern noise: PRNU and DSNU.

PRNU: Photo-Response Non-Uniformity is the variation of pixel output voltage across the image sensor array in the presence of uniform light. This is a result of non-uniformities in the circuitry itself. PRNU can be estimated via the slope pixel output value vs. illumination.

DSNU: Dark-Signal Non-Uniformity the presence of a non-zero pixel output value in the absence of light, and is the result of photodiode leakage and sensor read circuitry. DSNU can be estimated by looking at the offset of the pixel output vs. illumination relationship.

Read Noise

Read noise is the noise generated by the electronics when electron counts are converted to voltages. This is in the absence of any light or thermal effects. Read noise is usually higher for CMOS sensors than CCDs, although there has been much improvement in CMOS sensors for the past 20 years [2]. A lower read noise indicates a lower discernible level of detail in the image.

Dark Noise

Dark current is the photodetector current when illumination is absent. It is caused by thermally generated electrons, which can be from several sources within the photodetector. This can be in the depletion region, due to defects or surface states or carrier thermal generation and diffusion in the neutral bulk. This effect increases with longer exposure times [2].

Noise Estimation Methods and Results

PRNU and DSNU

To estimate the PRNU and DSNU, we work with raw images taken with the Google Pixel 4a image sensor using a uniform light field. Specifically, these images were taken using an integrating sphere to ensure that light rays reaching the image sensor span all angles uniformly. These images were taken for several exposure times, listed below. For each exposure time, several frames were taken.

Exposure Time (s)
0.0282
0.0336
0.0400
0.0476
0.0565

Table 1: List of exposure times

This process was repeated to capture images for several different ISO speeds.

ISO Speed
55
99
198
299
395
798

Table 2: List of ISO speeds

Sample raw images corresponding to one frame for each exposure time taken with ISO speed 55 are shown in Figure 1 below:

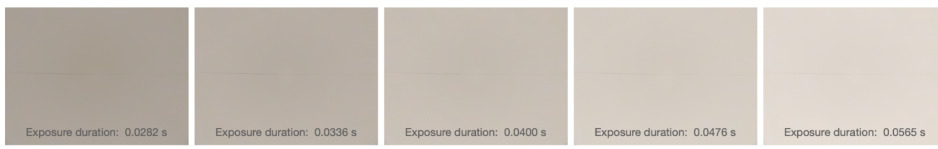

Sample Images for ISO speed 55

Figure 1: Sample Images

An overview of the process used to estimate the PRNU and DSNU of the image sensor from the raw images is given in the diagram below.

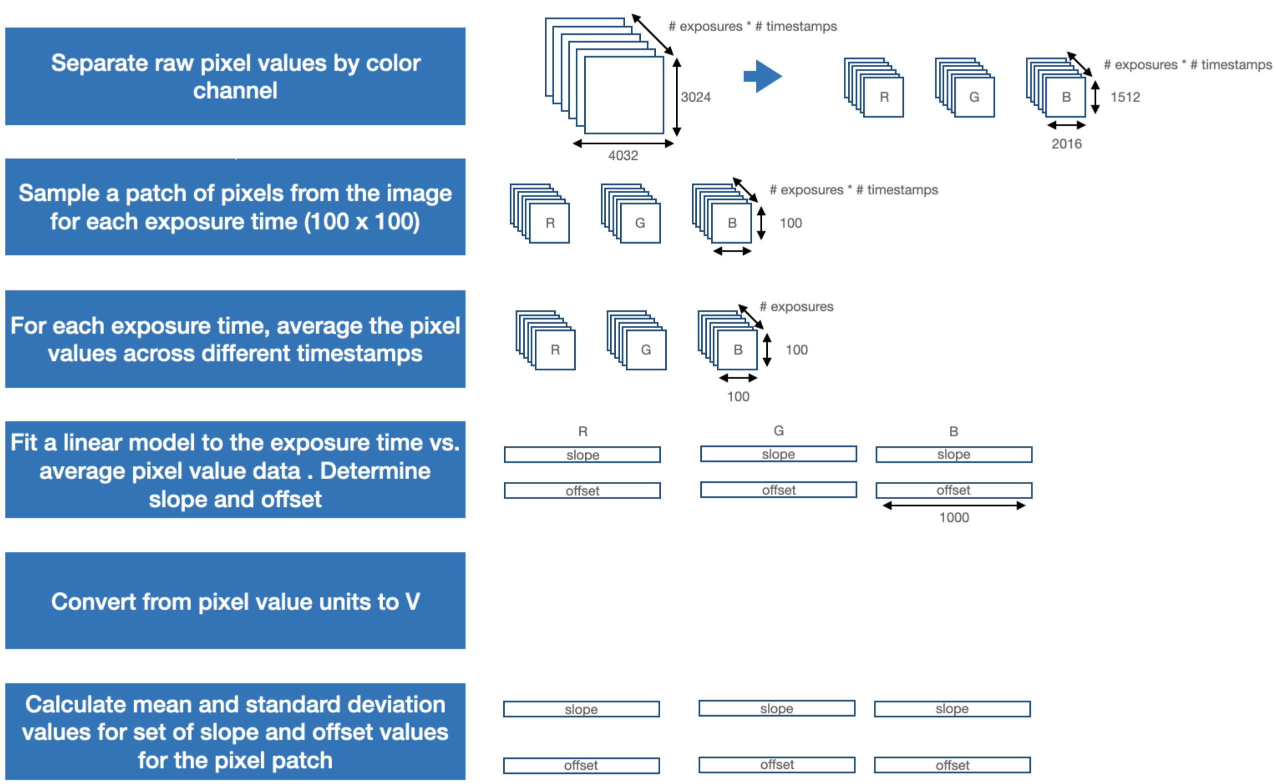

Figure 2: PRNU and DSNU estimation process

We first start by separating the raw images, loaded from DNG files, by color channel. Since the IMX363 sensor makes use of the standard Bayer color filter, we separate color channels by sampling pixels from every other row and every other column. We utilize the upper left pixel in each superpixel block in our analysis of the green channel.

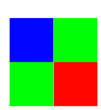

Figure 3: Bayer color filter

For each color channel and for each ISO speed we repeat the following process. We sample a patch of pixels for each frame and exposure time. This patch of pixels is arbitrarily sized 100 pixels by 100 pixels, which provides a large enough number of pixels to analyze the PRNU and DSNU distributions, but covers a small enough area so that comparison by location is meaningful. To reduce the effects of temporal noise in our estimation, we then average pixel values across images of the same exposure time. This allows us to plot the relationship between pixel value and exposure time for each pixel in the selected block. We fit a linear model to this relationship to estimate slope and offset values. A sample plot of pixel value vs. exposure time for ISO speed 55, and pixel location (1,1) for the red color channel is shown below.

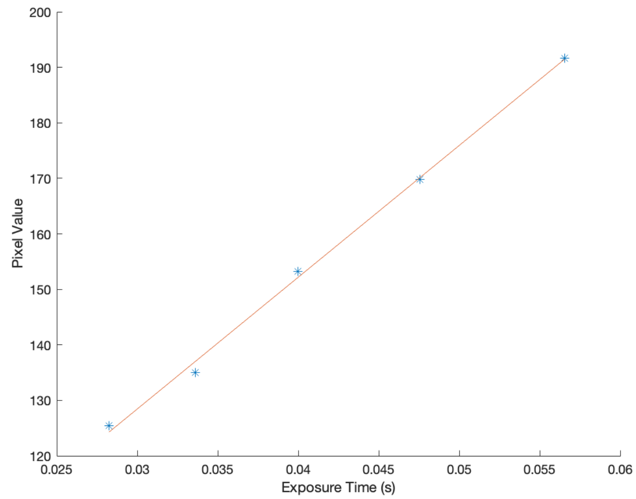

Figure 4: Pixel value vs exposure time, ISO speed 5, red color channel, pixel location (1,1)

Repeating this process for each of the pixels in the block provides 1000 slope and offset estimates which can be converted to units of V/s and V. To do so, we use the output voltage swing, which is 0.459. This results in the formula:

$$V = \frac{(pixel\ value)*0.459}{(2^{10}-1)}$$

The distribution of slope and offset values can be used to characterize the PRNU and DSNU of the sensor. The PRNU percentage is computed as the ratio of the standard deviation of the slope to the mean of the slope. The DSNU value is computed as the standard deviation of the offset.

The distributions of slope and offset values are visualized for each ISO speed in the histograms below in Figure 5 and 6 respectively. These correspond to the 100 x 100 pixel block located at [1, 100, 1, 100].

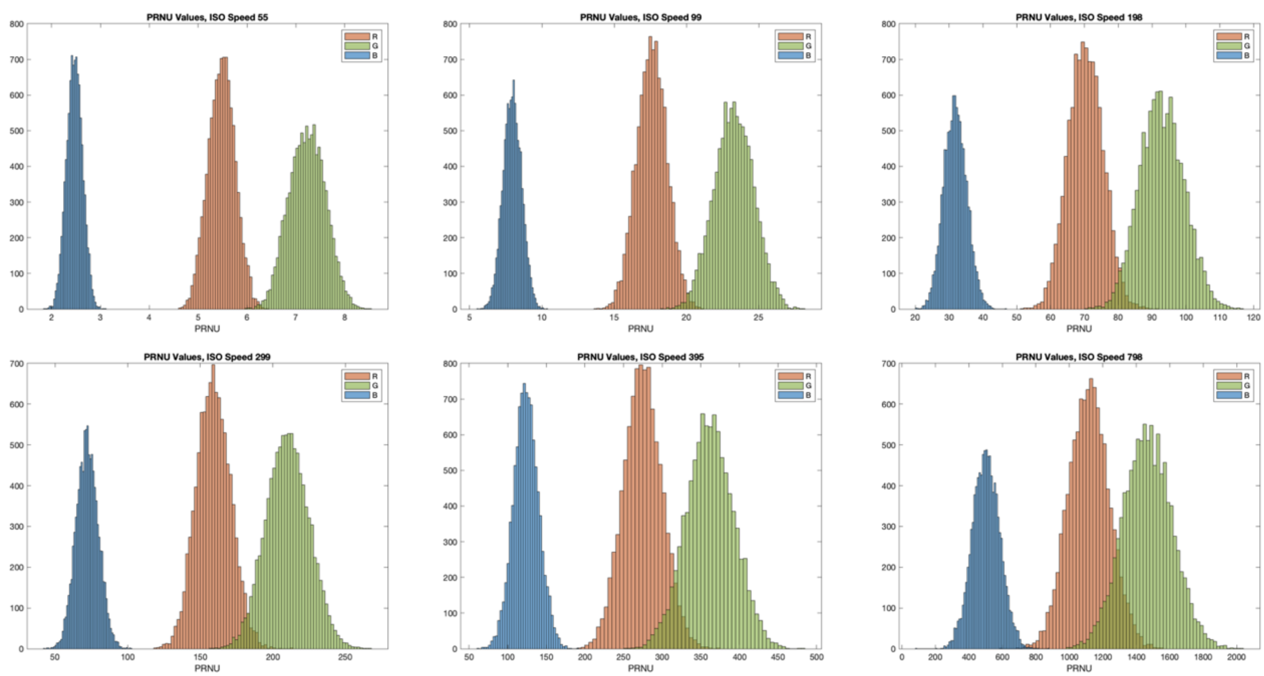

Figure 5: Slope values representing PRNU for pixel block at [1, 100, 1, 100]

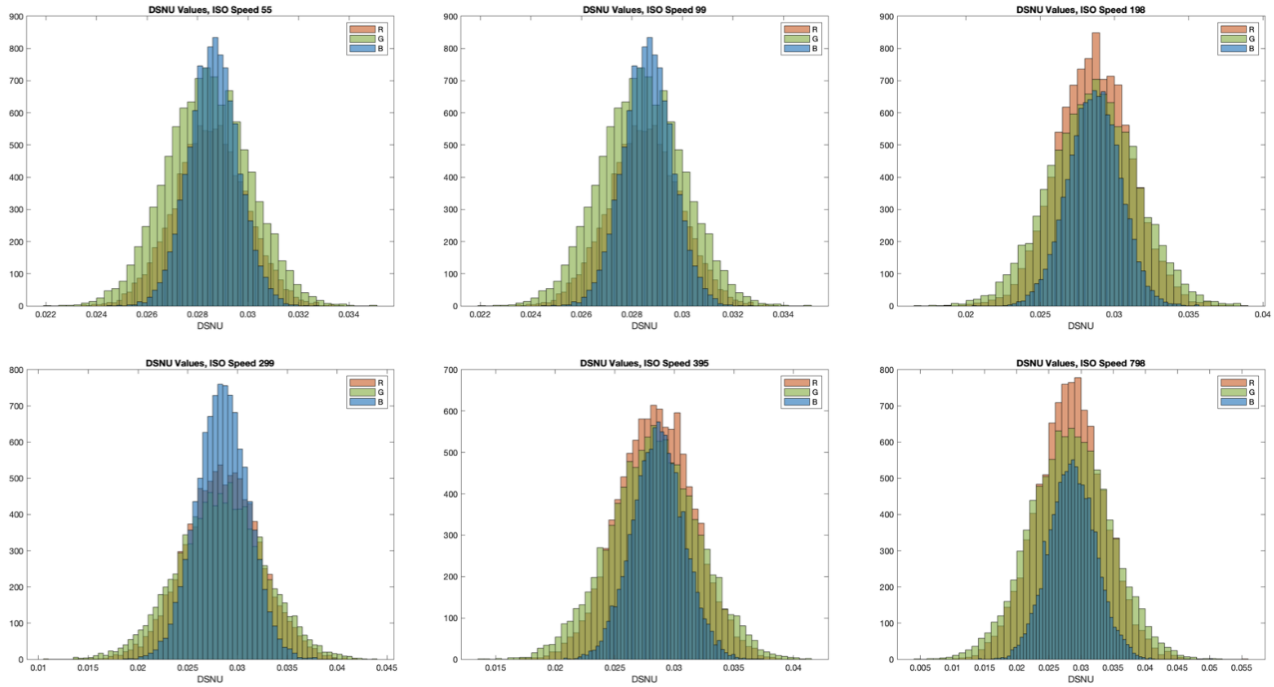

Figure 6: Offset values representing DSNU for pixel block at [1, 100, 1, 100]

We can see that the three color channels form three separate distributions with three distinct means for PRNU and share one mean but have varying distribution standard deviations for DSNU. As ISO speed increases, the red and green channel distributions for PRNU increasingly overlap.

To compare PRNU and DSNU across image sensor locations, we repeated the computations for a pixel block at [700, 800, 700, 800]. The slope and offset distributions for this pixel block are visualized below. We can see that the slope distribution have noticeable smaller standard deviations than the previous pixel block.

Slope:

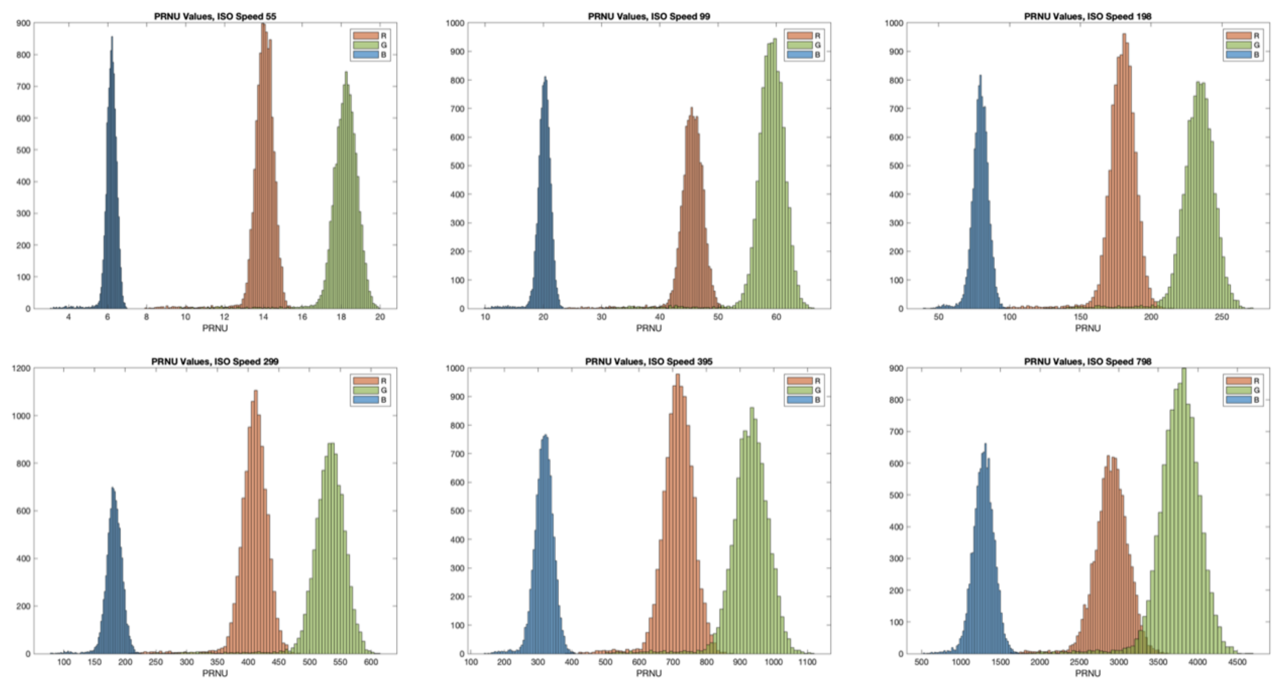

Figure 7: Slope values representing PRNU for pixel block at [700, 800, 700, 800]

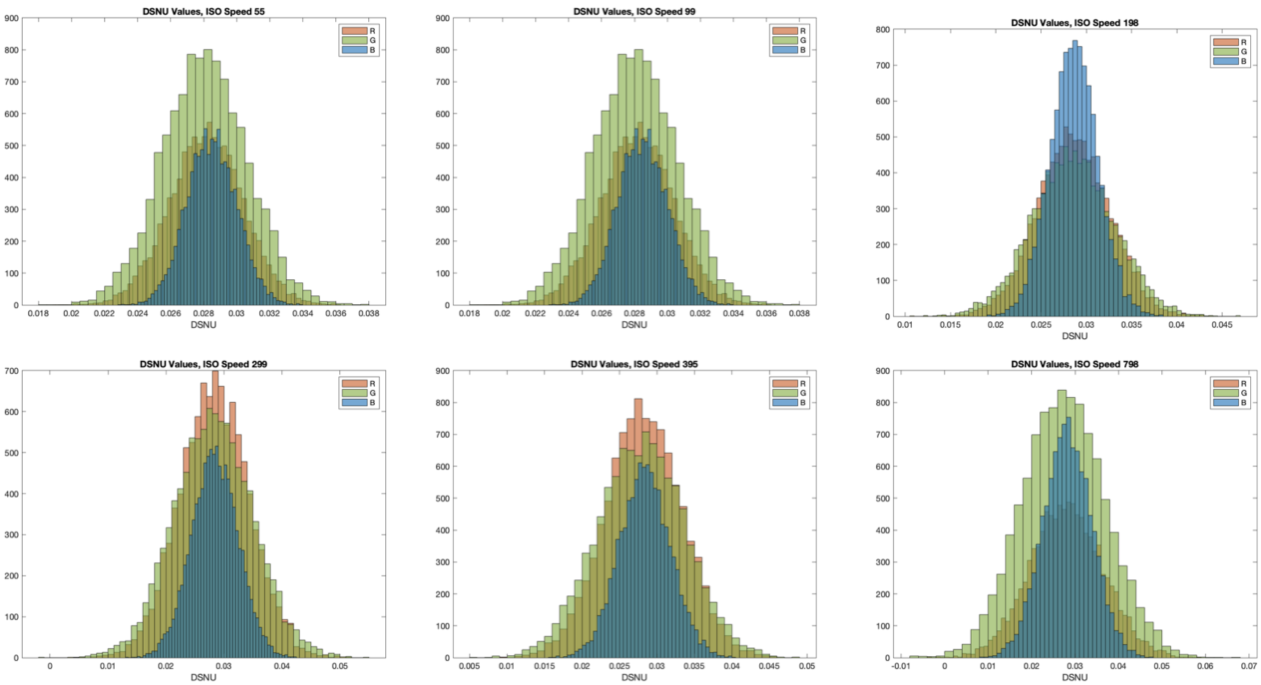

Figure 8: Offset values representing DSNU for pixel block at [700, 800, 700, 800]

The final estimated values for PRNU % and DSNU are tabulated below.

Pixel block at (1,1):

ISO Speed	R	G	B
55	4.981	5.115	6.601
99	5.924	5.858	8.017
198	7.299	6.972	10.611
299	7.360	7.018	10.578
395	9.013	8.476	13.157
798	10.871	10.030	16.258

Pixel block at (700,700):

ISO Speed	R	G	B
55	4.679	4.801	5.457
99	5.343	5.355	6.405
198	6.031	5.621	7.348
299	6.074	5.942	7.678
395	6.634	6.406	8.977
798	7.611	7.187	10.458

Table 3: Final estimated values of PRNU and DSNU

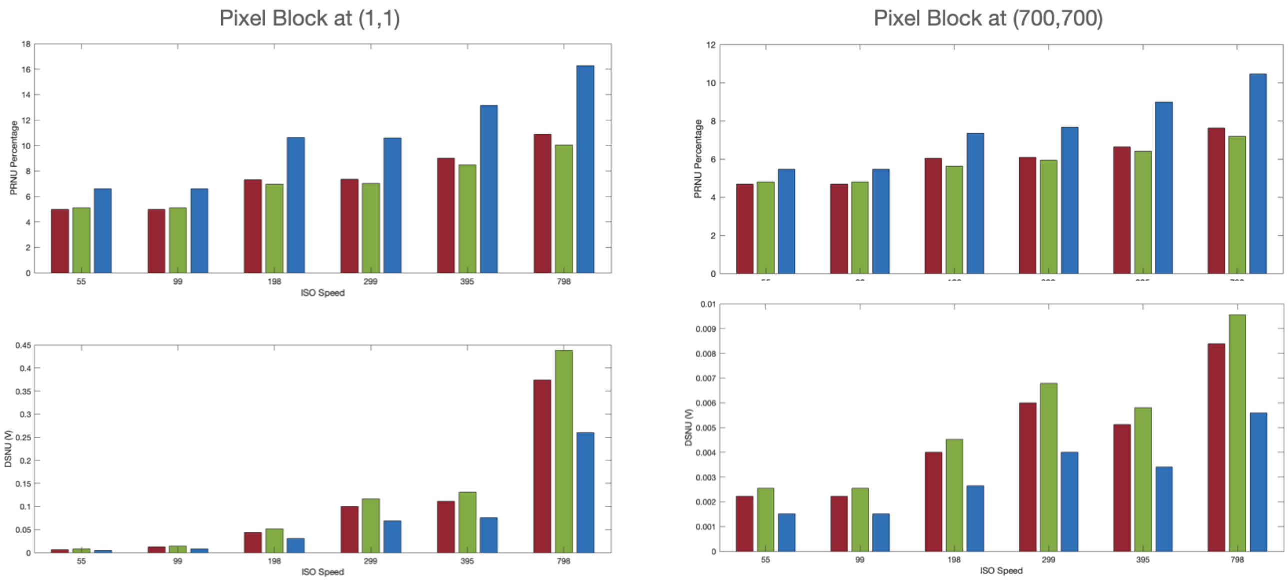

Figure 9: Final estimated values of PRNU and DSNU

We can see that the pixel block closer to the center produces, across all color channels, lower PRNU percentages and higher DSNU values. It can also be seen that as a whole, higher ISO speeds lead to larger PRNU percentages and higher DSNU values. Across color channels, the blue color channel mostly has the highest PRNU percentages and the green channel has the highest DSNU values.

Read noise

Read noise is the amount of noise generated by the electronics when electron counts are converted to voltages. In order to determine read noise, images were taken in the dark, at a very short exposure. This ensures that there is no photon noise, fixed pattern noise and dark shot noise is minimal. In the dataset there were 5 or 6 images (with the same settings) for each ISO speed. Since lens shading is not significant for an image taken in the dark, we used the whole image to estimate the read noise. For each image we converted the digital pixel values to voltages. This was done using the same voltage conversion used in fixed pattern noise calculations. Note we have not compensated for the differing gain used for different ISO values in this calculation, so we expect that higher ISO values will have a higher read noise.

We then separated the image into four arrays, one for each bayer block color. This enabled the RMS noise to be calculated for each color channel, where we considered each green pixel separately (to give R, G1, G2 and B channels). G1 and G2 were the two green pixels in the Bayer block and these were considered separately so that we could determine if there was any difference between the two color channels.

We calculated the standard deviation of all the voltages values across the each separated color entire image. This gave a set of standard deviations for each color channel and ISO value. These were averaged to a more precise value of the standard deviation (which is equivalent to the RMS noise value) for each ISO value and color channel.

Figure 10 shows a histogram of the noise values for ISO 798. The fitted normal distribution for each value is also displayed, which shows quite a good fit. It is also noted that there are some values which are much higher or lower than the standard deviation than would be expected of a normal distribution. It is suggested that this could be shot noise, but it is rare enough that it has a negligible impact on the statistics.

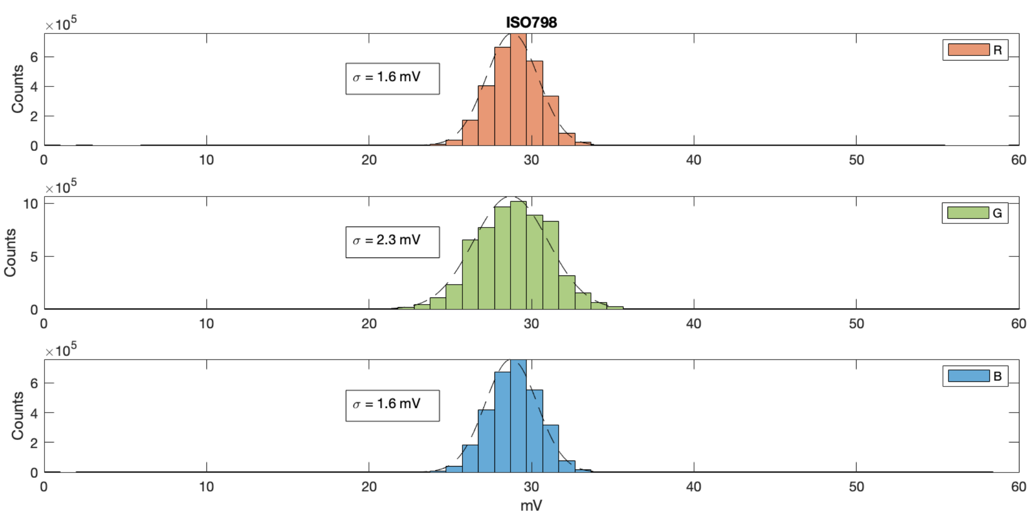

Figure 10: Histograms of noise distributions for ISO798

Figure 11 shows the relationship between the read noise and the ISO value. There is a linear relationship, as a higher ISO indicates a higher analog gain, which would amplify the read noise. The blue and red pixels have a very similar trend, however the green pixels (G1 and G2) have a higher noise by a factor of √2. G averaged is the average of each G1 and G2 pixel in each Bayer block. G averaged has a noise trend similar to the blue and red pixels. This is expected as there will be a reduction in the standard deviation after averaging. The std noise is reduced by a factor of the square root of the number of averages, which in this case is two, giving a factor of √2. It is suggested that the camera designers allowed for a higher read noise in the green pixels, as after averaging the two green responses, all colors will have a similar read noise in each Bayer block.

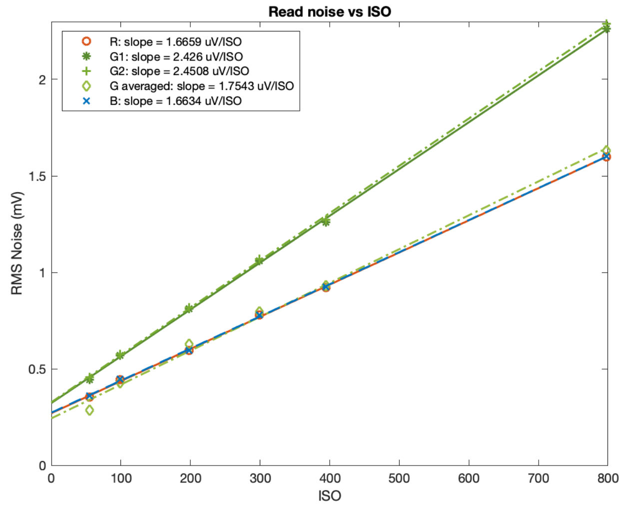

Figure 11: Read noise vs ISO for R, G (2 green elements averaged in each Bayer limit), G1, G2 and B

Table 4 shows the raw voltage values for the data in Figure x. We used an average across the different color channels to give an estimate of the noise for different ISO speeds in our model.

ISO	R (mV)	G1 (mV)	G2 (mV)	G averaged (mV)	B (mV)
55	0.354	0.445	0.457	0.284	0.358
99	0.444	0.570	0.574	0.429	0.447
198	0.594	0.812	0.819	0.627	0.595
299	0.777	1.060	1.070	0.794	0.778
395	0.922	1.259	1.273	0.931	0.924
798	1.600	2.262	2.288	1.629	1.601

Table 4: Read noise raw voltages for R, G (2 green elements averaged in each Bayer limit), G1, G2 and B

Dark Noise

The dataset includes images taken in the dark at various ISO values (55, 99, 198, 299, 395 and 798) and exposures (0.01, 0.02, 0.04, 0.08, 0.16 s). Since these images were taken in the dark, lens shading is minimal so we used the entire image for our calculations. To estimate the dark noise we calculate the mean voltage value of each pixel (separated by color channel) of each image. This mean value is plotted against the exposure time as in Figure 12. The gradient of the line of best fit gives the dark voltage in volts/second. This process was repeated for all color channels (R, G and B) and different iso speeds. We also tested the dark noise on smaller patches, but found the overall trends were less consistent than using the whole image.

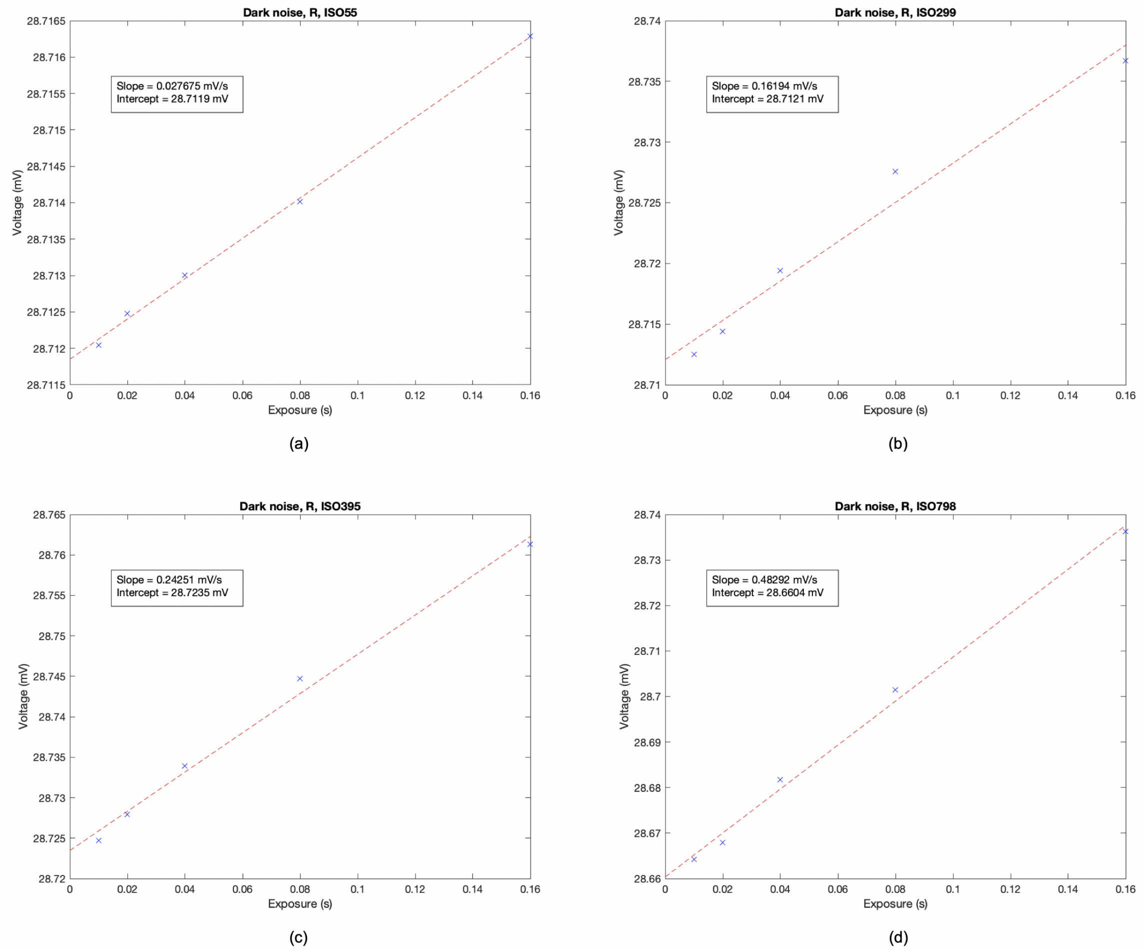

Figure 12: Dark noise growth on the Red color channels at (a) ISO 55, (b) 299, (c) 395 and (d) 798

Figure 13 shows the dark noise for each of the color channels across various ISO values. It can be seen that the dark noise increases with ISO value, and does not seem to depend significantly on color channel. The increase is due to the fact that we did not directly account for the different analog gain that would be used for the different ISO values in our measurements.

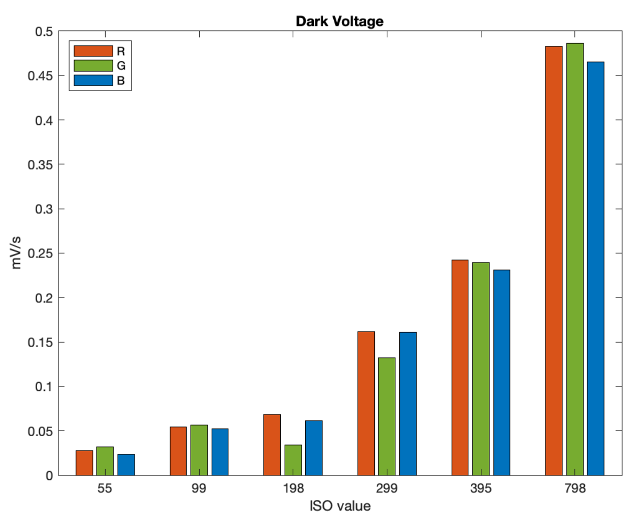

Figure 13: Dark noise for each ISO value when calculated across the whole image

Table 5 shows the raw data for Figure x.

ISO Speed	R (mV)	G (mV)	B (mV)
55	0.0277	0.0317	0.0238
99	0.0543	0.0566	0.0523

198	0.0685	0.0342	0.0612
299	0.1619	0.1319	0.1608
395	0.2425	0.2395	0.2313
798	0.4829	0.4865	0.4654

Table 5: Raw data for dark noise for each ISO value when calculated across the whole image

Sensor Model and Results

We use ISETCam, particularly the sensorCreate and sensorSet functions, to instantiate a model of the IMX363 sensor we analyzed and model test images using the estimated noise values for each ISO speed. For comparison of noise, we use two different scenes to simulate camera noise: a uniform white scene and a Macbeth chart to visualize the effects of camera noise on different colors. Below, the images produced by the simulated model for three different ISO speeds are shown.

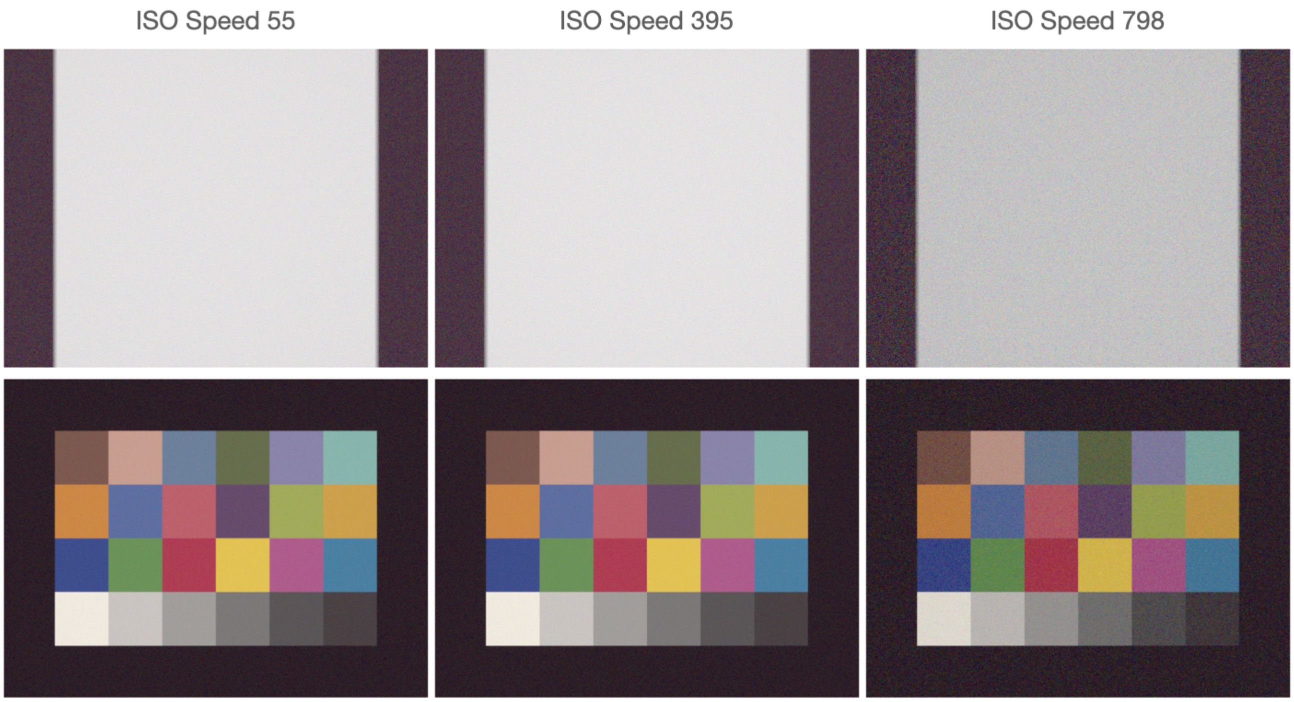

Figure 14: Sensor model outputs

Conclusion

In this project, we were able to produce estimates of four types of sensor noise- PRNU, DSNU, dark noise, and read noise- using DNG files produced using the Google Pixel 4a camera. From these estimates, we were able to draw comparisons of various noise levels across the three color channels as well as between different locations in the image. We were also able to characterize the correlation between noise levels and ISO speed for this image sensor. Using these estimated values, we successfully simulated models of the IMX363 image sensor that capture the noise levels at a particular ISO speed and visualize the output image at each ISO speed. This provides visual examples of the effects of noise levels on resulting images due to increasing ISO speed.

References

[1] J. Farrell and B. Wandell, ISETCAM, (2020), GitHub repository, https://github.com/iset/isetcam/wiki

[2] A. El Gamal and H. Eltoukhy, "CMOS image sensors," in *IEEE Circuits and Devices Magazine*, vol. 21, no. 3, pp. 6-20, May-June 2005, doi: 10.1109/MCD.2005.1438751.

Appendix

Code used in this project can be found at: https://github.com/mb2532/PSYCH221_FinalProject.git